

Current Limiting Simulation of Magneto-biased Superconducting Fault Current Limiter (SFCL) Applied in 66kV/10kV Power Substation in China

Qingshan Wang, Jiahui Zhu, Jialiang Liu, Yitao Liu, Defu Wei, Nan Zheng, Panpan Chen, Hongjie Zhang, Kaizhong Ding and Ercan Ertekin

Abstract—The short-circuit fault currents in the large capacity transmission lines pose a challenge to the stability and safety of power system. Magneto-biased superconducting fault current limiter (MBSFCL) is with the advantages of two-stage current limiting, self-triggering and fast recovery so that it can effectively reduce the short-circuit fault current when applied to the urban power system. This paper analyzes the operation principle of MBSFCL and establishes a package type magneto-thermal coupled simulation model of MBSFCL based on MATLAB/SIMULINK. A power system model of a 66 kV/10 kV Zhang Tai Zi power substation which is in Liaoning province in China has been established and the grid-connected simulation applied MBSFCL has been achieved. Moreover, the grid-connected test is carried out, and the results of fault current, quench resistance and temperature change are obtained. The comparison of results between simulation and test verifies the accuracy of the simulation model and the application feasibility of MBSFCL.

Index Terms—Magneto-biased superconducting fault current limiter (MBSFCL); fault current limiting rate; magneto-thermal coupled; simulation; substation

I. INTRODUCTION

With the continuous increase of transmission line capacity, the problem of short-circuit current is becoming more and more serious. Superconducting Fault Current Limiter (SFCL) has the advantages of fast current limiting response and low loss. It is an effective solution to the problem of short-circuit current.

In the past twelve years, a number of studies have been conducted on SFCL. In 2004, the Nexans company developed a three-phase 10 kV/10 MVA double-strand resistance type superconducting current limiter [1]. In 2010, the Korea Electric Power Company had carried out the test operation of the

Manuscript is submitted on 12, Nov., 2022. This work was supported by China State Grid Corporation Science and Technology Project under Grant DG71-22-006. (Corresponding author: Jiahui Zhu.)

Qingshan Wang, Jiahui Zhu, Jialiang Liu, Panpan Chen and Hongjie Zhang are with the China Electric Power Research Institute, Beijing, 100192, China (e-mail: 1045145027@qq.com).

Yitao Liu, Defu Wei and Nan Zheng are with the State Grid Liaoning Electric Power Company, Shenyang, 110006, China (e-mail: Liuyitao-71@sohu.com).

Kaizhong Ding is with the Institute of Plasma Physics Chinese Academy of Sciences, Hefei, 230031, China (e-mail: kzding@ipp.ac.cn).

Ercan Ertekin is with the University of Strathclyde, Glasgow, Scotland, G11 1XQ, United Kingdom (e-mail: ercan.ertekin@strath.ac.uk).

22.9 kV/0.63 kA hybrid superconducting current limiter [2]. In 2013, a 11 kV/10 MVA SFCL and a 11 kV/30 MVA SFCL were put to use in Birmingham, UK [3]. In 2019, this group had designed and tested a proof-of-principle 45 kVA, 450/450 V, single phase superconducting transformer with the fault tolerant capability [4]. In 2020, an improved algorithm has been presented to reduce the impact of resistive-SFCL for fault location [5]. In the same year, a novel SFCL was proposed as a power flow controller [6].

However, those above traditional SFCLs have a long quench recovery period, and requires a large amount of superconducting materials. It is unacceptable of them to meet the cost requirements for application in low-voltage lines. Therefore, the SFCL needs further improvement in reliability and economy. In this paper, a design and an application simulation of a magneto-biased superconducting fault current limiter (MBSFCL) in a 66 kV/10 kV power substation have been given. Moreover, the grid-connected tests have been achieved to validate the feasibility of MBSFCL in the power grids.

II. DESIGN OF MBSFCL

A. Topology and Parameters

The topology of MBSFCL is shown in Fig. 1. It includes a double-split reactor (L_1 and L_2), a superconducting non-inductive component (SNIC) and two fast switches (K_1 and K_2). The winding L_2 is series with K_1 , SNIC and K_2 . The two windings L_1 and L_2 of the double-split reactor are with high coupling coefficient, equal inductance values, and a reverse connection at the same ends. The SNIC is wound with Yttrium Barium Copper Oxide (YBCO) tapes and it has ten non-inductive superconducting units in series. The parameters of SNIC are shown in Table I.

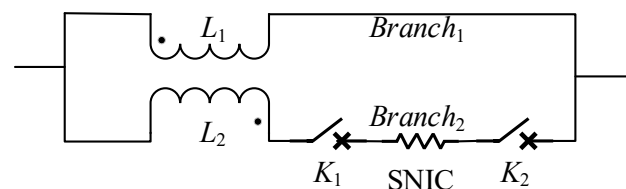


Fig. 1. The topology and components of MBSFCL.

TABLE I
PARAMETERS OF THE SNIC

Width of superconducting tape (mm)	Total length of superconducting tape (m)	Critical current of superconducting tape (A@77K)	Resistance at room temperature (mΩ)
4.8	232	100	4.56

B. Operation Principle

The operation of MBSFCL can be separated into four stages:

Steady-state operation: Fig. 2(a) describes that I_2 is less than the critical current of YBCO tapes. K_1 and K_2 are switched off. $I_1 = I_2$, thus the self-inductance of L_1 and L_2 has cancelled each other out. The impedance of MBSFCL reaches a low point.

First-stage current limiting: Fig. 2(b) describes that I_2 exceeds the critical current of YBCO tapes. YBCO tapes generate quench resistance R_{YBCO} , thus both I_1 and I_2 are on longer unequal and the self-inductance of L_1 and L_2 is no longer cancelled each other out. As a result, the impedance of MBSFCL will increase steeply to limit the fault current.

Second-stage current limiting: Fig. 2(c) describes that I_2 exceeds 200 A and lasts 10 ms. K_1 and K_2 are switched on. $Branch_2$ is cut off and $I_2 = 0$. The impedance of MBSFCL is the self-inductance of L_1 . The impedance of MBSFCL reaches a peak point in this circumstance.

Quench recovery: When both K_1 and K_2 are switched on. Because of the Joule heat accumulating before, YBCO tapes are in quenching state. They will be cooled by the cooling system until superconducting state can be recovered again to, so that MBSFCL can be put into the next operation.

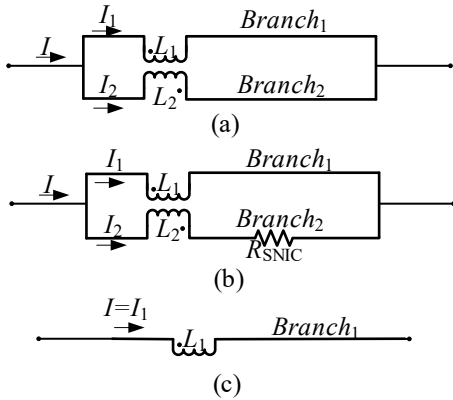


Fig. 2. The topology of MBSFCL in different stages: (a) steady-state operation (the current of SNIC is less than the critical current, thus R_{SNIC} is approximately equal to 0, and it does not appear in the figure); (b) first-stage current limiting; (c) second-stage current limiting.

C. Piecewise Model of Quench Resistance

The quench resistance of YBCO is a nonlinear function affected by the coupling of electric-magnetic-thermal fields. It is inaccurate to calculate the resistance change in the whole quench process only by a single quench characteristic value (n).

In this paper, a piecewise model is used to calculate the quench resistance [7]. According to the proportional relation-

ship between current density (J) and critical current density (J_c) of YBCO tapes, the quenching process is equivalent to a plurality of sections D ($D=1, 2, 3, \dots$).

The general expression of superconducting quench resistivity can be present by (1).

$$\rho_D(J) = \begin{cases} 0 & |J| < J_D \\ \frac{E_0}{|J|} \left(\frac{|J|}{J_c} - D \right)^{n_D} & |J| \geq J_D \end{cases} \quad (1)$$

where ρ_D , J_D and n_D are the quench resistivity, the critical current density and the quench characteristic value in different sections respectively. E_0 is the electric field corresponding to the critical current, which can be obtained from the critical current curve of YBCO tapes.

Under the impact of short-circuit current, YBCO tapes are in the rapid quenching state. The temperature T per unit length of YBCO tapes changes from T_0 to T_1 in time t , which can be calculated by (2).

$$T_1 - T_0 = \frac{I^2 R_{YBCO} t - h A_s (T_0 - T_{op}) t}{mc} \quad (2)$$

where I is the effective value of current. h is the surface heat transfer coefficient of tapes. A_s is the heat transfer area. R_{YBCO} is the overall resistance of tapes. m is the mass of unit length tapes. c is the specific heat coefficient of tapes.

III. GRID-CONNECTED SIMULATION APPLIED MBSFCL

A. Simulation Model of MBSFCL

The simulation model of MBSFCL is illustrated in Fig. 3. The superconducting non-inductive component is simulated by the S-Function module to control the controllable resistance module R_{sc} .

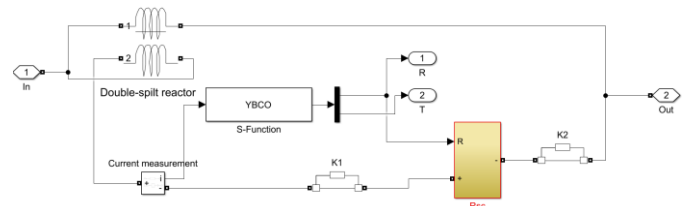


Fig. 3. The structure of simulation model of MBSFCL. The quench resistance is calculated by Matlab programming in the S-Function module.

B. Parameters of 66/10kV Power Substation

The simulation uses parameters of the line of 66 kV/10 kV Zhang Tai Zi power substation and its topology can be described in Fig. 4. There is a total of 7 nodes in the line, and the length of the whole line is 5.08 km, including a 0.482 km cable and a 4.598 km overhead line. The maximum conveying capacity is 5.455 MVA. All parameters of the line are shown in Table II. There are two main loads in the line, one node 16 is a clothing factory with active power 1.051 MW and reactive

power 0.233 MVar, and the other node 62 is a steel rolling mill with active power 0.29 MW and reactive power 0.178 MVar. MBSFCL is installed at 20m from the transformer outlet.

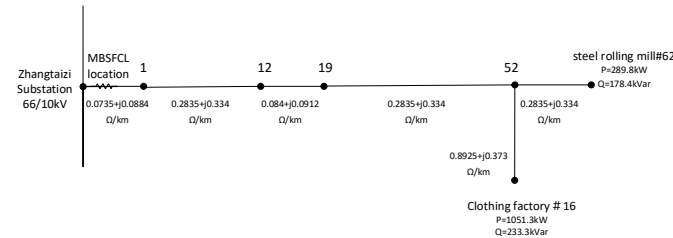


Fig. 4. The topology of the line of 66 kV/10 kV power substation.

TABLE II
PARAMETERS OF THE LINE

Zone	Wire type	Wire Ristance(Ω/km)	Wire inductance (mH/km)	length (km)
0-1	YJV22-3*300	0.0735	0.2817	0.1
1-12	LGJ-120	0.27	1.0828	0.7
12-19	YJV22-3*240	0.084	0.2904	0.46
19-62	LGJ-120	0.27	1.0828	2.15
52-16	LGJ-35	0.8925	1.1879	0.85

C. Simulation Results and Analysis

Set the fault point at node 52, and the fault type is three-phase short-circuit. The simulation duration is 0-0.3 s. the fault start time is 0.1 s, and the stop time is 0.2 s. The liquid nitrogen is used as cooling medium.

Define the current limiting rate k is (3)

$$k = (i_0 - i_1) / i_0 \times 100\% \quad (3)$$

where i_0 is the 2nd peak value of fault current without MBSFCL. i_1 is the 2nd peak value of fault current with MBSFCL.

The overall trends of the three phases are all the same, so phase A can be an example to analysis.

When the line is without MBSFCL, the current waveforms are shown in Fig. 5(a). The normal current is about 108.1 A. The 1st peak value of fault current is 2500.2 A, and the 2nd peak value of fault current is 2330.3 A. When the line is connected with MBSFCL, the current waveforms are shown in Fig. 5(b). The normal current is at the same level about 108.1 A. The 1st peak value of fault current is 2336.0 A, and the 2nd peak value of fault current is 1880.2 A. It can be calculated that the current limiting rate is 19.32 %.

The quench resistance waveform of MBSFCL before and after the fault starts is shown in Fig. 6, and the temperature waveform is shown in Fig. 7. The maximum quench resistance is 1.07 Ω. The maximum temperature is 123.7 K. According to the time the highest temperature declined to 77 K, the quench recovery time is 32 ms.

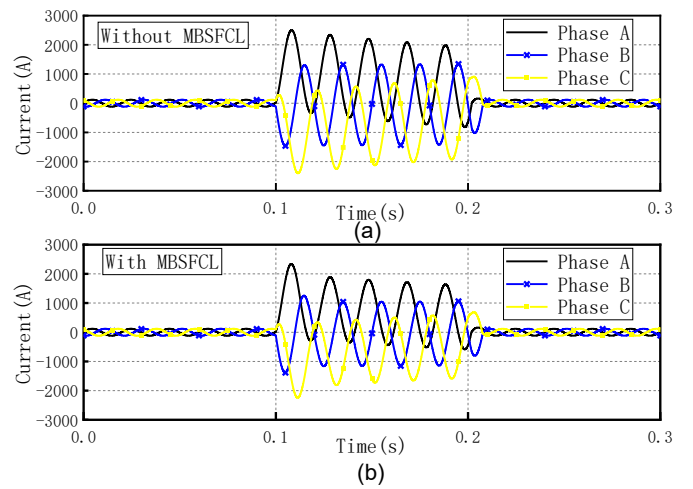


Fig. 5. The fault current of line: (a) without MBSFCL; (b) with MBSFCL.

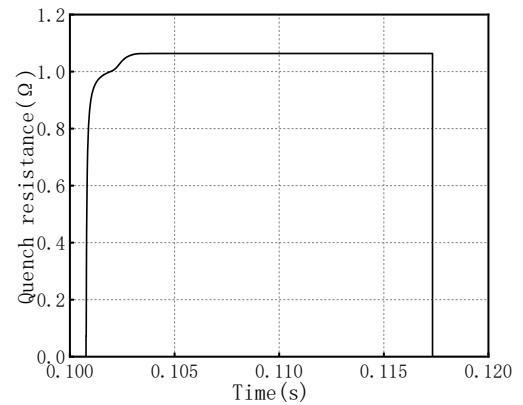


Fig. 6. The quench resistance of MBSFCL of Phase A.

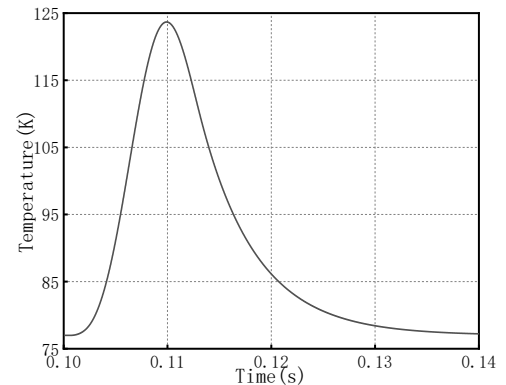


Fig. 7. The temperature of MBSFCL of Phase A.

IV. GRID-CONNECTED TEST APPLIED MBSFCL

A. General Situation of Grid-connected Test

In grid-connected test, the MBSFCL has been connected in series with phase B transmission line in 66kV/10kV Zhang Tai Zi power substation. And this test has lasted for 7 days. The photo of grid-connected test of MBSFCL is shown in Fig. 8. Fig. 9(a) is the interface of MBSFCL system, and Fig. 9(b) is the interface of cooling system.



Fig. 8. The photo of site of grid-connected test.

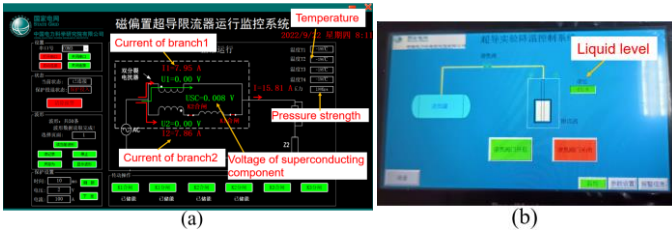


Fig. 9. The interface of MBSFCL system and cooling system: (a) the MBSFCL system; (b) the cooling system.

B. Fault Current Limiting Test

It is necessary to conduct fault current limiting test for proving the current limiting ability of MBSFCL and the accuracy of the simulation model. The fault type of this test is AB two-phase interphase short-circuit. The fault duration is 10 ms. The fault start time is 0.1 s, and other conditions are the same as the simulation.

The current waveform of phase B is shown in Fig. 10. When MBSFCL is connected, the 1st peak value of fault current is 1715 A, and the 2nd peak value of fault current is 998 A. And when MBSFCL is disconnected, the 1st peak value of fault current is 1650 A, and the 2nd peak value of fault current is 845 A. Consequently, the current limiting rate is 15.33 %.

The voltage waveform of the superconducting component is shown in Fig. 11. According to the fluctuation of voltage waveform, the quench recovery time is 40 ms.

The quench resistance waveform is shown in Fig. 12. There is a noise around 1.023 s, which should be ignored. The maximum quench resistance is 0.97 Ω .

Table III shows the results comparison between simulation and grid-connected test. It can be found that the simulation results are close to the test results, and the difference range is no more than 20%.

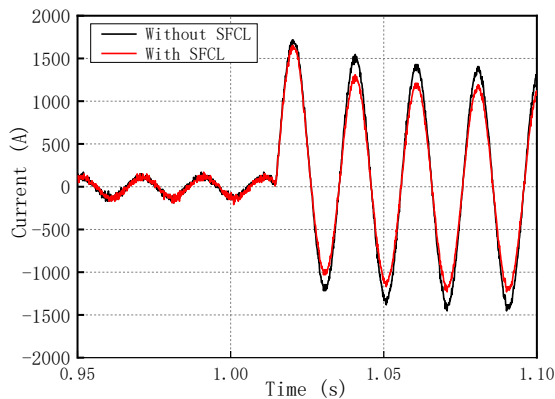


Fig. 10. The current waveform of phase B.

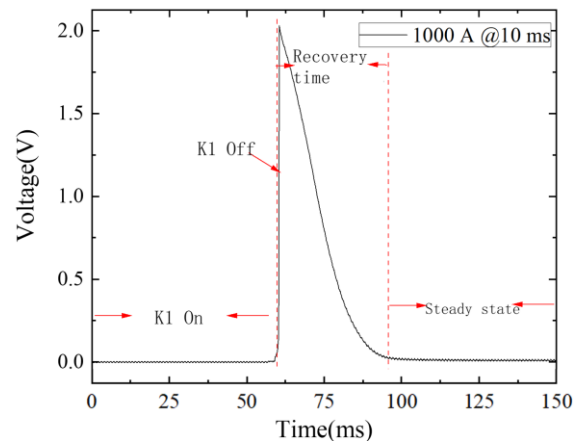


Fig. 11. The voltage waveform of the superconducting component.

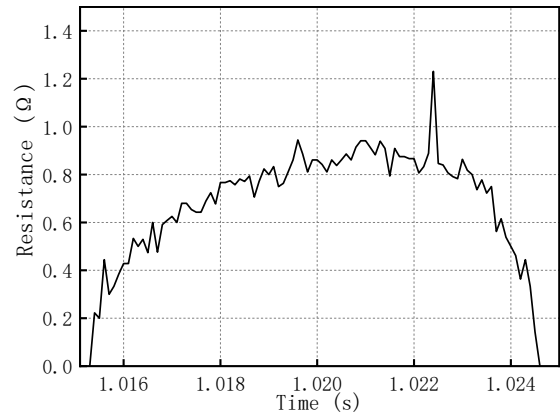


Fig. 12. The resistance waveform of the superconducting component.

TABLE III
RESULTS COMPARISON

Result types	Current limiting rate	Maximum quench resistance(Ω)	Quench recovery time(ms)
Simulation	19.32 %	1.07	32
Grid-connected test	15.33 %	0.97	40

V. CONCLUSION

This paper proposes a design of MBSFCL and finishes the fault current limiting simulations. The grid-connected test applying MBSFCL has been achieved and we successfully measure the relevant parameters of MBSFCL, the test results verify the current limiting effect of MBSFCL in 66 kV/10 kV Zhang Tai Zi power substation and explore the feasibility of its application.

REFERENCES

- [1] R. Kreutz, J. Bock, F. Breuer, et al., "System technology and test of CURL 10, a 10 kV, 10 MVA resistive high-Tc superconducting fault current limiter," *IEEE Trans. Appl. Supercond.*, vol. 15, no. 2, pp. 1961-1964, June 2005.
- [2] Amir Heidary, Hamid Radmanesh, Kumars Rouzbehi, et al., "Long-Term Operation and Fault Tests of a 22.9 kV Hybrid SFCL in the KEP-

- 1 CO Test Grid," *IEEE Trans. Appl. Supercond.*, vol. 21, no. 3, pp. 2131-
2 2134, June 2011.
- 3 [3] "Grid ON's Fault Current Limiter commissioned into service by ETI at
4 a UK Power Networks substation," Energy Technol. Inst., Loughbor-
5 ough, U.K., Accessed: Jun. 6, 2013. [Online]. Available:
6 [http://www.eti.co.uk/gridons-fault-current-limiter-successfully](http://www.eti.co.uk/gridons-fault-current-limiter-successfully-suppresses-multiple-network-faults-during-first-year-in-service/) suppress-
7 es-multiple-network faults-during-first-year-in-service/
8 [4] Yazdani-Asrami, M, Staines, M, Sidorov, G, et al., "Fault current limit-
9 ing HTS transformer with extended fault withstand time," *SUPERCON-*
10 *DUCTOR SCIENCE & TECHNOLOGY*, vol. 32, no. 3, Mar. 2019, Art
11 no. 035006.
- 12 [5] Guillen D, Salas C, Trillaud F, Castro LM, et al., "Impact of Resistive
13 Superconducting Fault Current Limiter and Distributed Generation on
14 Fault Location in Distribution Networks," *Electric Power Systems Re-*
15 *search*, vol. 186, Sept 2020, Art no. 106419.
- 16 [6] A. Heidary, H. Radmanesh, K. Rouzbehi and H. Moradi CheshmehBeigi,
17 "A Multifunction High-Temperature Superconductive Power Flow Con-
18 troller and Fault Current Limiter," *IEEE Trans. Appl. Supercond.*, vol.
19 30, no. 5, Aug. 2020, Art no. 5601208.
- 20 [7] J. Zhu, Y. Zhao, P. Chen, et al., "Magneto-Thermal Coupling Design
21 and Performance Investigation of a Novel Hybrid Superconducting Fault
22 Current Limiter (SFCL) With Bias Magnetic Field Based on
23 MATLAB/SIMULINK," *IEEE Trans. Appl. Supercond.*, vol. 29, no. 2,
24 March 2019, Art no. 5601405.
- 25
26
27
28
29
30
31
32
33
34
35
36
37
38
39
40
41
42
43
44
45
46
47
48
49
50
51
52
53
54
55
56
57
58
59
60